

Relationship between electrical and optical characterization of Ga-doped ZnO thin films deposited by magnetron sputtering

Trang Thuy Thi Phan^{1,2}, Anh Tuan Thanh Pham^{1,2,*}, Thang Bach Phan^{1,2,3}, Vinh Cao Tran^{1,2}



Use your smartphone to scan this QR code and download this article

¹Laboratory of Advanced Materials, University of Science, Ho Chi Minh City, Vietnam

²Vietnam National University, Ho Chi Minh City, Vietnam

³Center for Innovative Materials and Architectures (INOMAR), Ho Chi Minh City, Vietnam

Correspondence

Anh Tuan Thanh Pham, Laboratory of Advanced Materials, University of Science, Ho Chi Minh City, Vietnam

Vietnam National University, Ho Chi Minh City, Vietnam

Email: pttanh@hcmus.edu.vn

History

- Received: 2022-12-02
- Accepted: 2023-03-21
- Published: 2023-04-15

DOI :

<https://doi.org/10.32508/stdj.v26i1.4024>



Copyright

© VNUHCM Press. This is an open-access article distributed under the terms of the Creative Commons Attribution 4.0 International license.



ABSTRACT

Introduction: Transparent conducting films have received much attention in energy conversion applications. To replace high-cost indium-tin-oxide (ITO), Ga-doped ZnO (GZO) film is considered due to its high conductivity, good transparency, low cost, and low toxicity. **Methods:** GZO and pure ZnO films were deposited on glass substrates by dc magnetron sputtering. The crystalline structure of the samples was verified by using X-ray diffraction. In particular, the relationship between the electrical and optical characterization of the GZO film was investigated through the plasma wavelength obtained from transmittance and reflectance spectra. Meanwhile, carrier transport was directly confirmed by Hall effect-based measurements. **Results:** The GZO film shows a hexagonal wurtzite structure, with successful incorporation of Ga into the ZnO lattice. Ga doping increases the carrier concentration, leading to a decrease in the resistivity of the film. This study also discusses the correlation of carrier transport obtained from Hall effect-based measurements and optical spectroscopies. Here, we extracted the optical carrier concentration and optical mobility from the plasma wavelength and compared them with the Hall data. **Conclusion:** The dependence of carrier transport on ionized impurity scattering can be pointed out. It proposes an effective way to qualitatively predict the electrical characteristics and transport properties of thin films via optical transmittance and reflectance analysis.

Key words: Ga-doped ZnO, thin films, plasma wavelength, magnetron sputtering

INTRODUCTION

Over the past few decades, transparent conducting oxide (TCO) films have been widely used for electrodes in optoelectronic applications such as thin-film transistors, organic light-emitting diodes, and flat solar cells¹. Indium-tin-oxide (ITO) has been the best TCO material due to its outstanding characteristics, such as low resistivity and high transparency in the visible range². However, ITO is expensive due to the scarcity of indium. ZnO has emerged as an alternative material for ITO because it has many advantages, such as a wide band gap semiconductor (3.37 eV), a high exciton binding energy (60 meV), low toxicity, low cost, and high thermal stability³. However, due to a low carrier concentration, pure ZnO normally has weak electrical conductivity. To improve the conductivity, the most commonly used approach is doping with IIIA-group elements, including Al, Ga, and In⁴. Among them, Ga-doped ZnO (GZO) is a promising candidate for good-performance TCO applications. Apart from high-cost deposition techniques, the GZO film deposited by magnetron sputtering exhibits some advantages, such as a relatively simple process, good uniformity, and high adhesion⁵.

In addition, analytical techniques are indispensable for investigating the electrical and optical characteristics of TCO films, specifically GZO films. Jo et al. used four-point probes and ultraviolet–visible (UV–Vis) spectra to study the resistance and transmittance of GZO films⁶. Mahdhi et al. investigated the thickness-dependent electrical and optical properties of films by using Hall effect-based measurements, and UV–Vis spectra were extended to the near-infrared (NIR) region⁷. In addition, current-voltage (J–V) characterization can also be employed to analyze carrier transport⁸. However, the relationship between optical and electrical signals through these analytical techniques has been less reported. Therefore, this study reports the optical-electrical relationship of the GZO film. Specifically, the electrical properties of the film are directly determined from Hall effect-based measurements and indirectly derived from the optical UV–Vis–NIR spectra. From the comparison, the carrier transport of the film can be estimated.

MATERIALS – METHODS

Pure ZnO and GZO films were prepared on glass substrates using dc magnetron sputtering (Leybold

Cite this article : Phan T T T, Pham A T T, Phan T B, Tran V C. Relationship between electrical and optical characterization of Ga-doped ZnO thin films deposited by magnetron sputtering. *Sci. Tech. Dev. J.*; 2023, 26(1):2659-2664.

Univex-450). The sputtering targets were self-produced from ZnO (99.9%, Merck) and Ga₂O₃ (99.99%, Sigma Aldrich) with an atomic ratio of Ga/Zn = 5/95. The powder mixture was blended with distilled water and then ball-milled for 5 hours. After that, the mixture was dried at 150°C for 24 hours and then pressed and sintered via solid-state reaction at 1400°C in air. Before loading into the sputtering chamber, the glass substrates were thoroughly cleaned in an ultrasonic bath for 15 minutes with a base, distilled water, and acetone solution to remove dust and numerous organic contaminants. Furthermore, the substrate surface was plasma-treated under an Ar pressure at 10⁻² Torr to clean the substrates and ensure uniformity and purity of the films. The base and working pressures were 4 × 10⁻⁶ Torr and 3.5 × 10⁻³ Torr, respectively. The substrate temperature and sputtering power were set at 300°C and 60 W, respectively. The thickness of the films was controlled at approximately 600 nm, corresponding to a deposition time of approximately 20 minutes.

The crystalline structure of the pure ZnO and GZO thin films was examined by using X-ray diffraction (XRD, Bruker D8-Advance). The experimental electrical parameters (carrier concentration, Hall mobility, and resistivity) of the GZO film were determined at room temperature by Hall effect-based measurements (Linseis HCS-1) with the Van der Pauw method. The optical transmittance and reflectance spectra of the films (substrate included) were recorded by using a UV-Vis-NIR spectrophotometer (Jasco V-770) with a wavelength region of 300–2700 nm.

RESULTS

Structural characterization

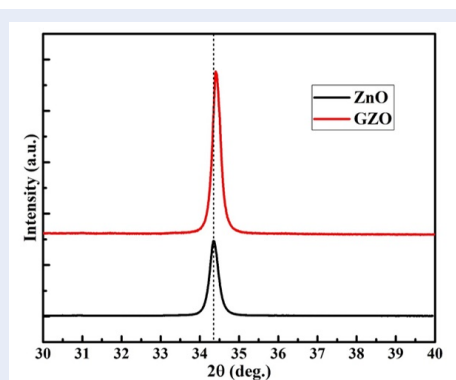


Figure 1: XRD pattern of the GZO film compared to the pure ZnO sample.

The crystalline structure of the GZO film is considered through the XRD patterns, as shown in Figure 1. A single peak is observed at the 2θ position of 34.40° for the GZO film, corresponding to the (002) plane of ZnO (JCPDS 36-1451). This suggests that the GZO film has a hexagonal wurtzite structure with a preferential c-axis orientation perpendicular to the substrate. No peak relating to the Ga₂O₃ phase is found, which implies the incorporation of Ga atoms in the ZnO matrix⁹. Specifically, the (002) plane of the GZO film shifts toward larger 2θ angles compared to the pure ZnO film (34.34°). According to Bragg's law, a larger 2θ angle is associated with a decrease in the interplanar spacing $d_{(002)}$ (as shown in Table 1), indicating the substitution of smaller-radius Ga³⁺ (0.068 nm) at Zn²⁺ sites (0.072 nm)¹⁰. In addition, the residual stress (ϵ) of the films can also be estimated from the 2θ position of the (002) plane, as given by $\epsilon = A(c - c_0)/c_0$, where $A = -232.8$ GPa is the elastic factor of ZnO, and c and c_0 are the lattice constants of the investigated films and stress-free powder¹¹. Both films have compressive stress due to the negative values (as shown in Table 1). Furthermore, the absolute ϵ value of the GZO film is much smaller than that of the pure ZnO film, indicating stress relaxation. Thus, the deformation of the ZnO structure can be effectively repaired by the substitution of Ga.

In addition, a higher diffraction intensity of the (002) plane is observed for the GZO film. This suggests the enhancement of the crystalline quality of the ZnO film by Ga doping. To support the improved crystalline quality, the mean crystal size (D) of the films is calculated by using the Scherrer equation¹², as given by $D = 0.9\lambda/\beta \cos\theta$, where $\lambda = 0.154$ nm is the X-ray wavelength, β is the full width at half maximum, and θ is the Bragg diffraction angle. The D -values are found to be 32.5 and 35.3 nm for the pure ZnO and GZO films, respectively. Thus, doping Ga improves the crystalline structure of the ZnO film.

Electrical properties

Electrical properties, including resistivity (r), carrier concentration (n), and mobility (μ) of the GZO film, are directly determined from the Hall effect-based measurements, as listed in Table 2. The GZO film shows n-type behavior, as confirmed by the negative Hall coefficient (R_H). Compared to pure ZnO, the strong reduction in resistivity of the GZO films results from increasing both the carrier concentration and mobility. The electrical properties obtained for the GZO film are also better than those of some previous reports^{13,14}. The conductivity of a pure ZnO film

Table 1: Crystallographic data of the GZO and pure ZnO films.

Samples	2θ (deg.)	d ₍₀₀₂₎ (nm)	c (nm)	ε (GPa)	D (nm)
Pure ZnO	34.34	0.2608	0.5217	-0.4475	32.5
GZO	34.40	0.2604	0.5208	-0.0537	35.3

Table 2: Electrical properties of the GZO and pure ZnO films.

Samples	R _H (10 ⁻² cm ³ /C)	n (10 ²⁰ cm ⁻³)	μ (cm ² /Vs)	r (10 ⁻³ Ωcm)	Λ (nm)
Pure ZnO	-9.34	0.7 ± 0.1	22.8 ± 0.7	4.1 ± 0.4	1.9
GZO	-1.09	4.9 ± 0.3	25.5 ± 1.0	0.50 ± 0.02	4.1

is normally relatively low, mainly dominated by the low carrier concentration generated from oxygen vacancies and zinc interstitials¹⁵. The incorporation of Ga can increase the carrier concentration of the GZO film. Concretely, Ga atoms can be ionized into Ga³⁺ at substitutional Zn²⁺ sites, thus contributing a free electron from each Ga atom. In addition, the mobility of the GZO films is also improved compared to the pure ZnO films and a previous study¹⁶.

From the Hall effect-based results, the effects of Ga doping on the electrical properties of ZnO films can include two aspects. First, Ga³⁺ can substitute Zn²⁺ sites in the ZnO lattice to produce donors and free electrons. This mainly contributes to the increased carrier concentration of the GZO film. Second, many defects can exist in the ZnO film, causing a large compressive stress in the pure ZnO film. The substitution of Ga can compensate for the defects (for example, zinc vacancies - V_{Zn}) and relax the stress. This is mainly responsible for the increased mobility of the GZO film. Additionally, the reduction in acceptor traps (V_{Zn}) also contributes to the carrier concentration. Consequently, the increases in the carrier concentration and mobility of the film are simultaneously attributed to Ga doping.

Furthermore, the mobility is disturbed by scattering mechanisms related to ionized impurities, lattice defects, and grain boundaries. To understand the carrier transport properties, the mean free path (Λ) of electrons can be evaluated by the following formula¹⁷:

$$\Lambda = \frac{h(3\pi^2n)^{1/3}\mu}{2\pi e}$$

where h is the Plank constant and e is the electronic charge. The results of Λ are also shown in Table 2. It is seen that the Λ-value of the GZO film is enhanced more than twofold relative to the pure ZnO film. This result also suggests an improvement in the crystalline quality of the GZO film. However, these values of Λ

are still much smaller than the mean crystal size calculated from the XRD data (Table 1). Consequently, the grain boundary scattering can be ignored, whereas the electronic scattering inside the crystalline grains becomes dominant. It will be considered later in the discussion section. Additionally, free-electron scattering can also decrease the mobility. However, the probability of electron-electron collisions was demonstrated to be very small in semiconductor materials at room temperature¹⁸. Thus, the effect of free-electron scattering on the mobility of the films can also be neglected.

Optical properties

Figure 2a shows the transmittance spectra of the GZO film in the wavelength region of 300–2700 nm. In the visible region, the film exhibits good transparency (~80%) with some interference fringes and a sharp absorption edge. In the UV region, the decrease in transmittance of the film may be due to the initiation of elementary absorption in this region or to the displacement of charge carriers in the internal energy region of the material^{19,20}. In the long wavelength region (>1000 nm), the transmittance of the film tends to decrease continuously. This can be explained by the change in plasma oscillation (plasma wavelength λ_p or frequency ω_p) proportional to the carrier concentration. Light with a higher wavelength than λ can be completely reflected.

According to theoretical and practical calculations, ZnO is a direct transition semiconductor; thus, the optical bandgap of the ZnO-base films can be determined by using Tauc's plot method²¹, as given by αhv² ~ hv - E_g, where α, h, v, and E_g are the absorption coefficient, Planck constant, frequency, and optical band gap, respectively. The optical bandgap of the GZO film is extrapolated from the straight-line portion of the curve to the zero absorption coefficient value, as shown in Figure 2b. The E_g value of

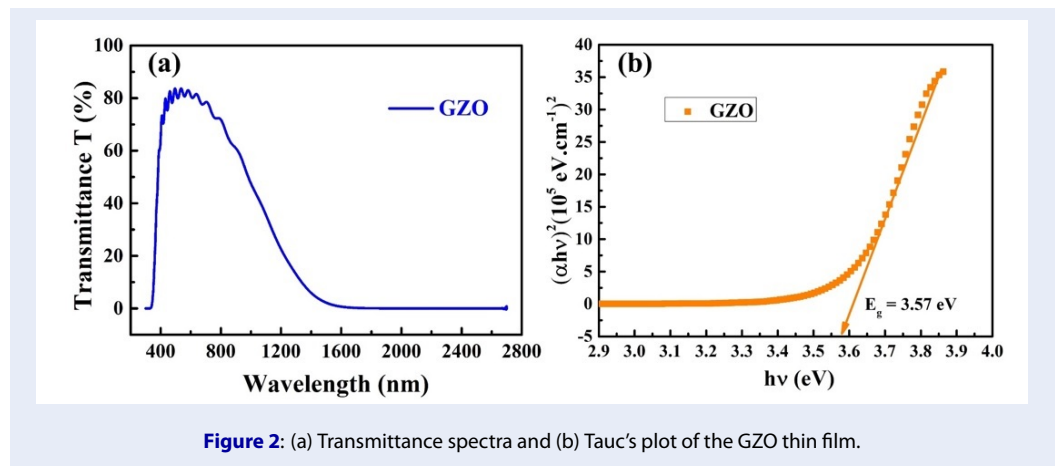


Figure 2: (a) Transmittance spectra and (b) Tauc's plot of the GZO thin film.

the film is found to be ~3.57 eV. According to previous reports, the band gap of pure ZnO films is normally equal to approximately 3.3 eV²². This demonstrates that the widening of the optical bandgap of the GZO film is explained by the Burstein-Moss effect²³, in which the higher the carrier concentration is, the larger the bandgap is. This result completely agrees with the carrier concentration obtained from the Hall effect-based measurements.

DISCUSSION

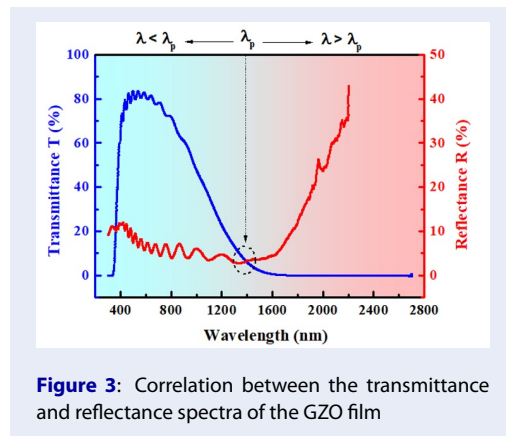


Figure 3: Correlation between the transmittance and reflectance spectra of the GZO film

The relationship between Hall effect-based measurement and optical spectroscopy in estimating the electrical properties of the GZO film is considered. Usually, when the electric field component of light interacts with the electrons inside the film, there are basic optical phenomena such as absorption, transmission, and reflection. Figure 3 shows the transmittance and reflectance spectra of the GZO film. Theoretically, if $\lambda > \lambda_p$, the films are as reflective as metals.

Otherwise, the films have high transmittance, similar to dielectrics. Therefore, λ_p is often determined at the frequency position where transmittance equals reflectance. Through the transmission and reflection spectra of the GZO film, the λ_p -value is found at the wavelength position of 1400 nm. From the plasma wavelength value, the optical carrier concentration (N_{opt}) can be calculated as follows²⁴:

$$N_{opt} = \frac{m^* \epsilon_0 \epsilon_\infty \omega_p^2}{e^2} = \frac{4\pi^2 c^2 m^* \epsilon_0 \epsilon_\infty}{e^2} \times \frac{1}{\lambda_p^2}$$

where m^* is the effective mass of electrons, c is the light speed, and ϵ_0 and ϵ_∞ are the permittivity of free space and the high-frequency permittivity of the material, respectively. Assuming $\epsilon_\infty = 4$ and $m^* = 0.23 m_o$, where m_o is the electron mass^{25,26}, we can estimate $N_{opt} = 5.2 \times 10^{20} \text{ cm}^{-3}$ for the GZO film. This value is approximate with the obtained carrier concentration from the Hall effect-based measurement ($4.9 \times 10^{20} \text{ cm}^{-3}$).

Apart from carrier concentration, a discussion on mobility is indispensable. As previously reported by Bruneaux et al.²⁷, a difference between optical mobility and Hall mobility values can be observed for ZnO-based films. It is noted that the carrier transport in materials under an electric field is restricted by grain boundary scattering, reducing Hall mobility²⁵. On the other hand, grain boundary scattering will not affect optical mobility; instead, scattering inside the grains can be dominant²⁸. However, in our GZO film, the mean free path of electrons is minimal compared to the mean crystal size, as shown in Tables 1 and 2. This suggests that grain boundary scattering has less effect on the carrier transport of the film. Indeed, the optical mobility is found to be equal to $23.8 \text{ cm}^2/\text{Vs}$, which is close to the Hall mobility (25.5

cm²/Vs). This confirms the dominant electronic scattering on ionized impurities instead of grain boundaries²⁹. Additionally, the inconsiderable differences in the carrier concentration and mobility determined from the Hall effect-based measurement and the optical spectra suggest an accurate assessment of the electrical properties of the GZO film.

CONCLUSION

Using the magnetron sputtering method, the resistivity of the obtained GZO film (5×10^{-4} Wcm) is one order lower than that of the pure ZnO sample, which is suitable for transparent electrode applications. This is a result of increasing both the carrier concentration and mobility of the film by doping Ga. The comparison between the Hall and optical mobilities indicates that the carrier transport is mainly governed by grain-boundary and ionized-impurity scattering mechanisms for the pure ZnO and GZO films, respectively. Consequently, this study suggests an effective way to accurately assess the electrical properties of transparent semiconducting films.

LIST OF ABBREVIATION

GZO: Ga-doped ZnO
MFP: Mean free path
XRD: X-ray diffraction

COMPETING INTERESTS

The authors declare that they have no competing interests.

AUTHOR CONTRIBUTION

Trang Thuy Thi Phan prepared the samples and wrote the draft. Anh Tuan Thanh Pham performed all the measurements and revised the manuscript. Thang Bach Phan supported the methodology and discussed the results. Vinh Cao Tran acted as a scientific supervisor and leader of the research group.

ACKNOWLEDGMENTS

This research is funded by Vietnam National University HoChiMinh City (VNU-HCM) under grant number VL2022-18-02.

Hall effect-based measurements (Linseis HCS-1) and UV-Vis-NIR (Jasco V-770) were carried out at the Center for Innovative Materials and Architectures, VNU-HCM.

REFERENCES

1. Kyu KS, Yun KD, Wan PJ, Rock SK, Geun KT. Work function-tunable ZnO/Ag/ZnO film as an effective hole injection electrode prepared via nickel doping for thermally activated delayed fluorescence-based flexible blue organic light-emitting

- diodes. Appl. Surf. Sci. 2021; 538: 148202; Available from: <https://doi.org/10.1016/j.apsusc.2020.148202>.
2. Sousa MG, da Cunha AF. Optimization of low temperature RF-magnetron sputtering of indium tin oxide films for solar cell applications. Appl. Surf. Sci. 2019; 484: 257-264; Available from: <https://doi.org/10.1016/j.apsusc.2019.03.275>.
3. Truong LOK, Thanh PAT, Pham NK, Cao PTH, Nguyen TH, Van HD, et al. Compensation of Zn substitution and secondary phase controls effective mass and weighted mobility in In and Ga codoped ZnO material. J. Mater. 2021; 7: 742-755; Available from: <https://doi.org/10.1016/j.jmat.2020.12.020>.
4. Sikam P, Moontragoon P, Ikonic Z, Kaewmaraya T, Thongbai P. The study of structural, morphological and optical properties of (Al, Ga)-doped ZnO: DFT and experimental approaches. Appl. Surf. Sci. 2019; 480: 621-635; Available from: <https://doi.org/10.1016/j.apsusc.2019.02.255>.
5. Chen Y, Meng F, Ge F, Xu G, Huang F. Ga-doped ZnO films magnetron sputtered at ultralow discharge voltages: Significance of controlling defect generation. Thin Solid Films 2018; 660: 840-845; Available from: <https://doi.org/10.1016/j.tsf.2018.03.019>.
6. Jo GH, Koh JH. Laser annealing effects on Ga dopants for ZnO thin films for transparent conducting oxide applications. Ceram. Int. 2019; 45: 6190-6197; Available from: <https://doi.org/10.1016/j.ceramint.2018.12.096>.
7. Mahdhi H, Alaya S, Gauffier JL, Djessas K, Ben Ayadi Z. Influence of thickness on the structural, optical and electrical properties of Ga-doped ZnO thin films deposited by sputtering magnetron. J. Alloys Compd. 2017; 695: 697-703; Available from: <https://doi.org/10.1016/j.jallcom.2016.11.117>.
8. Alobaidi OR, Chelvanathan P, Bais B, Sopian K, Alghoul MA, Akhtaruzzaman M, et al. Vacuum annealed Ga:ZnO (GZO) thin films for solar cell integrated transparent antenna application. Mater. Lett. 2021; 304: 130551; Available from: <https://doi.org/10.1016/j.matlet.2021.130551>.
9. Lee CS, Lee BT, Jeong SH. In-depth study on defect behavior and electrical properties in Ga-doped ZnO films by thermal-treatment under different chemical equilibrium. J. Alloys Compd. 2020; 818: 152892; Available from: <https://doi.org/10.1016/j.jallcom.2019.152892>.
10. Pham ATT, Hoang DV, Nguyen TH, Truong LOK, Wong DP, Kuo J-L, et al. Hydrogen enhancing Ga doping efficiency and electron mobility in high-performance transparent conducting Ga-doped ZnO films. J. Alloys Compd. 2021; 860: 158518; Available from: <https://doi.org/10.1016/j.jallcom.2020.158518>.
11. Truong LOK, Pham ATT, Nguyen TH, Hoang DV, et al. Impacts of Ga doping on the structural and thermoelectric properties of ZnO bulks sintered by solid-state reaction. Sci. Technol. Dev. J. 2022; 25: 2432-2438;.
12. Holzwarth U, Gibson N. The Scherrer equation versus the &Debye-Scherrer equation": Nat. Publ. Gr. 2011; 6: 534; PMID: 21873991. Available from: <https://doi.org/10.1038/nnano.2011.145>.
13. Ponja SD, Sathasivam S, Parkin IP, Carmalt CJ. Highly conductive and transparent gallium doped zinc oxide thin films via chemical vapor deposition. Sci. Rep. 2020; 10: 638; PMID: 31959884. Available from: <https://doi.org/10.1038/s41598-020-57532-7>.
14. Appani SK, Singh D, Nandi R, Sutar DS, Major SS. Influence of oxygen partial pressure on the strain behavior of reactively cosputtered Ga doped ZnO thin films. Thin Solid Films 2023; 764: 139624; Available from: <https://doi.org/10.1016/j.tsf.2022.139624>.
15. Hjiri M, Aida MS, Lemine OM, El Mir L. Study of defects in Li-doped ZnO thin films. Mater. Sci. Semicond. Process. 2019; 89: 149-153; Available from: <https://doi.org/10.1016/j.mssp.2018.09.010>.
16. Bruncko J, Šutta P, Netrvalová M, Michalka M, Vincze A. Pulsed laser deposition of Ga doped ZnO films - Influence of deposition temperature and laser pulse frequency on structural,

- optical and electrical properties. *Vacuum* 2019; 159: 134-140; Available from: <https://doi.org/10.1016/j.vacuum.2018.10.031>.
17. Pham DP, Nguyen HT, Phan BT, Hoang VD, Maenosono S, Tran CV. Influence of addition of indium and of postannealing on structural, electrical and optical properties of gallium-doped zinc oxide thin films deposited by direct-current magnetron sputtering. *Thin Solid Films* 2015; 583: 201-204; Available from: <https://doi.org/10.1016/j.tsf.2015.03.068>.
 18. Kittel C. *Introduction to solid-state physics*. (John Wiley & Sons, Inc., 2004);
 19. Misra P, Ganeshan V, Agrawal N. Low temperature deposition of highly transparent and conducting Al-doped ZnO films by RF magnetron sputtering. *J. Alloys Compd.* 2017; 725: 60-68; Available from: <https://doi.org/10.1016/j.jallcom.2017.07.121>.
 20. Inamdar SI, Rajpure KY. High-performance metal-semiconductor-metal UV photodetector based on spray deposited ZnO thin films. *J. Alloys Compd.* 2014; 595: 55-59; Available from: <https://doi.org/10.1016/j.jallcom.2014.01.147>.
 21. Li J, Zhu X, Xie Q, Yang D. Surface nanosheets evolution and enhanced photoluminescence properties of Al-doped ZnO films induced by excessive doping concentration. *Ceram. Int.* 2019; 45: 3871-3877; Available from: <https://doi.org/10.1016/j.ceramint.2018.11.059>.
 22. Barnasas A, Kanistras N, Ntagkas A, Anyfantis DI, Stamatiatos A, Kapaklis V, et al. Quantum confinement effects of thin ZnO films by experiment and theory. *Phys. E Low-Dimensional Syst. Nanostructures* 2020; 120: 114072; Available from: <https://doi.org/10.1016/j.physe.2020.114072>.
 23. Kaushal A, Kaur D. Effect of Mg content on structural, electrical and optical properties of Zn1-xMgxO nanocomposite thin films. *Sol. Energy Mater. Sol. Cells* 2009; 93: 193-198; Available from: <https://doi.org/10.1016/j.solmat.2008.09.039>.
 24. Saha M, Ghosh S, Ashok VD, De SK. Carrier concentration dependent optical and electrical properties of Ga doped ZnO hexagonal nanocrystals. *Phys. Chem. Chem. Phys.* 2015; 17: 16067-16079; PMID: 26029747. Available from: <https://doi.org/10.1039/C4CP05480F>.
 25. Steinhauser J, Faÿ S, Oliveira N, Vallat-Sauvain E, Ballif C. Transition between grain boundary and intragrain scattering transport mechanisms in boron-doped zinc oxide thin films. *Appl. Phys. Lett.* 2007; 90: 142107; Available from: <https://doi.org/10.1063/1.2719158>.
 26. Xu CX, Sun XW, Chen BJ. Field emission from gallium-doped zinc oxide nanofiber array. *Appl. Phys. Lett.* 2004; 84: 1540-1542; Available from: <https://doi.org/10.1063/1.1651328>.
 27. Bruneaux J, Cachet H, Froment M, Messad A. Correlation between structural and electrical properties of sprayed tin oxide films with and without fluorine doping. *Thin Solid Films* 1991; 197: 129-142; Available from: [https://doi.org/10.1016/0040-6090\(91\)90226-N](https://doi.org/10.1016/0040-6090(91)90226-N).
 28. Steinhauser J, Meyer S, Schwab M, Faÿ S, Ballif C, Kroll U, et al. Humid environment stability of low pressure chemical vapor deposited boron doped zinc oxide used as transparent electrodes in thin film silicon solar cells. *Thin Solid Films* 2011; 520: 558-562; Available from: <https://doi.org/10.1016/j.tsf.2011.06.095>.
 29. Fan Y, Zheng W, Zhu S, Cheng L, Qi H, Li L, et al. Extraction of carrier concentration and mobility of ZnO by mid-infrared reflectance spectroscopy. *J. Lumin.* 2021; 239: 118365; Available from: <https://doi.org/10.1016/j.jlumin.2021.118365>.